



Supplement of

Vehicle-based in situ observations of the water vapor isotopic composition across China: spatial and seasonal distributions and controls

Di Wang et al.

Correspondence to: Di Wang (di.wang@lmd.ipsl.fr) and Lide Tian (ldtian@ynu.edu.cn)

The copyright of individual parts of the supplement might differ from the article licence.

1 I. Figures

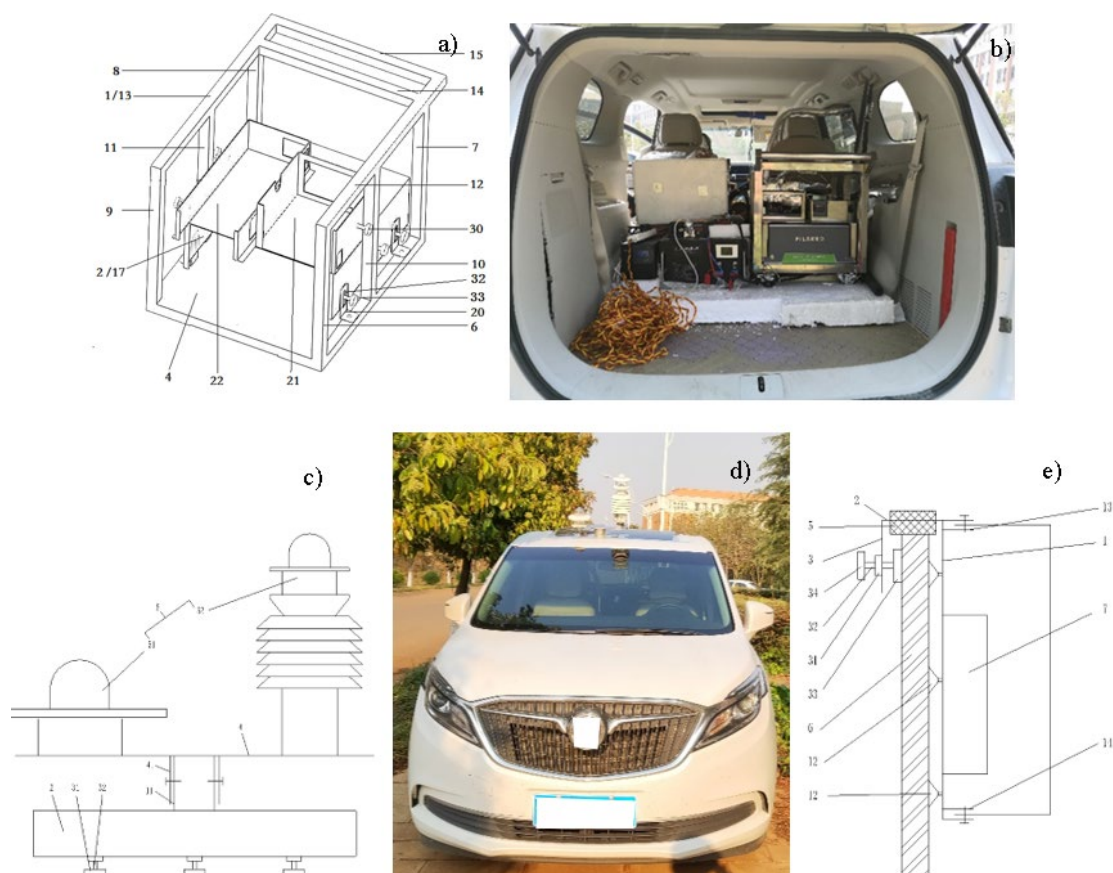


Fig.S1 The design diagram (a) and real product (b) of vehicle-borne mobile water vapor isotope observation device, the design diagrams of the mobile weather station based on car skylight (c) and off-vehicle detection mount platform (e). The location of the vapor isotopes sampling inlet and measurement instrument on the car (d).

The design diagrams can be found in the published patents as following:

1. Di Wang, Qin Liu, Lide Tian. A vehicle-borne mobile water vapor isotope observation device: China, ZL201921098630.1. 2020-02-19. (in Chinese)
2. Di Wang, Xiaobo Sun, Lide Tian, Xuejie Wang, Mingxing Tang. A Mobile Weather Station Based on Car Skylight: China, ZL201921357774.4. 2020-01-16. (in Chinese)
3. Di Wang, Lide Tian, Mingxing Tang, Xuejie Wang. An off-vehicle detection mount platform: China, ZL201921355641.3. 2020-01-10. (in Chinese)

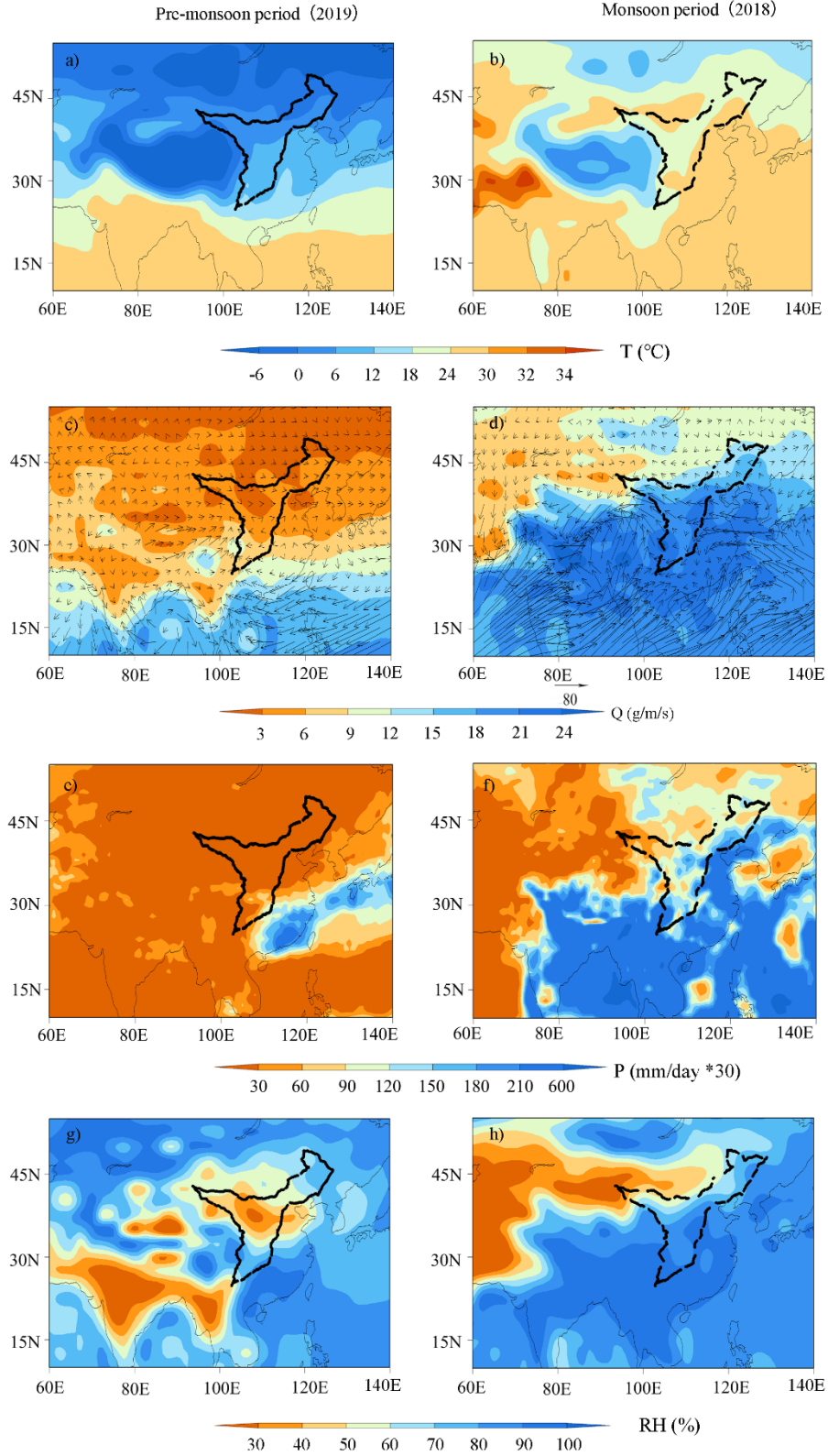


Fig.S2 The temporal-mean surface air temperature T (°C, a and b), the vertically-integrated moisture flux from the surface to an altitude of 300 hpa Q (g/m/s, c and d) (Connolley and King, 1993), precipitation amount P (mm/day *30, e and f), and surface relative humidity RH (% , g and h) for the sampling dates. The left panel is for the pre-monsoon period and the right for the monsoon period.

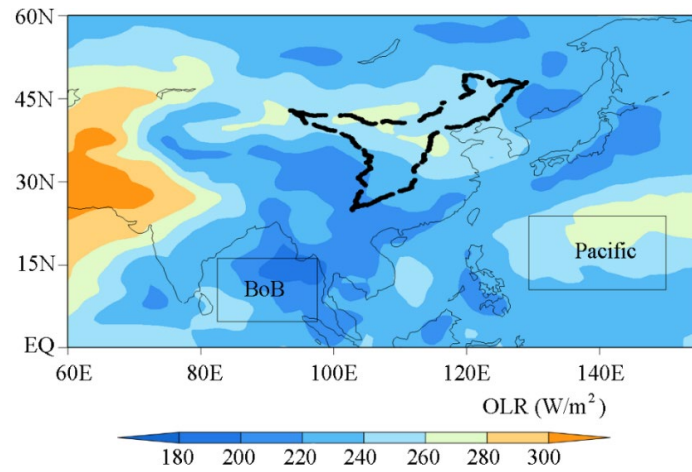


Fig.S3 Spatial distribution of monthly outgoing longwave radiation (OLR, W/m²) in August 2018. Note: BoB is the abbreviation for the Bay of Bengal.

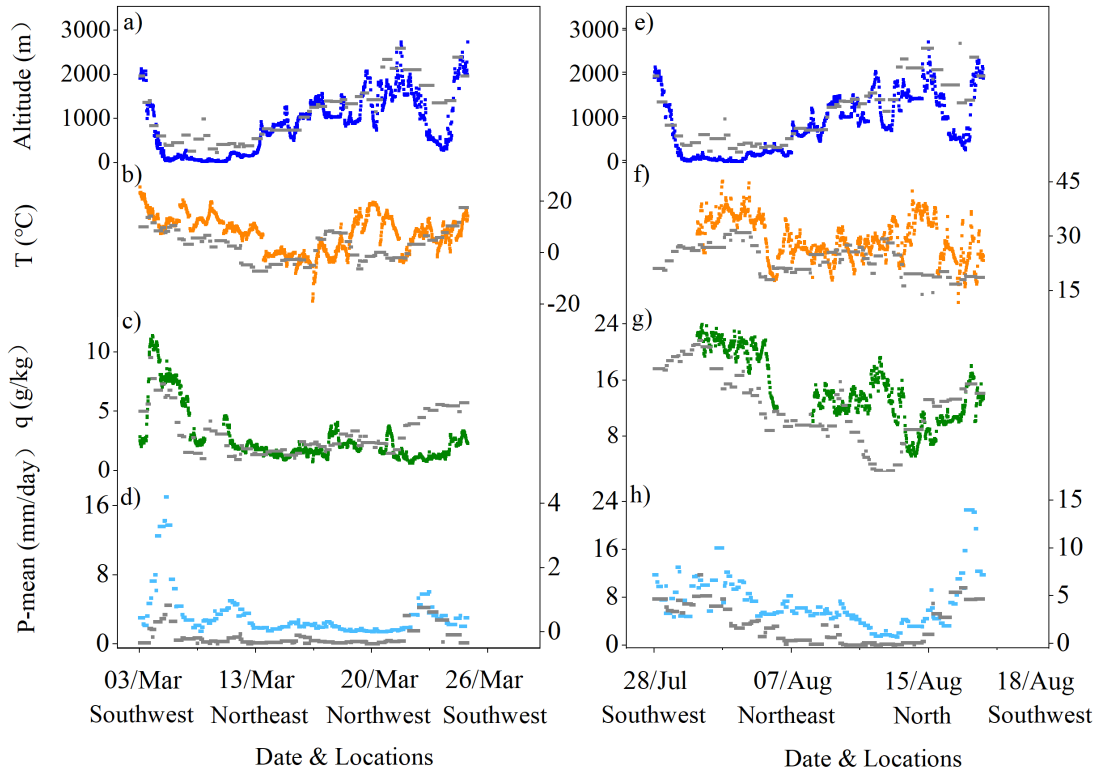


Fig.S4 Concurrent meteorological conditions along the survey routes of observations (colourful dots) and simulations of Iso-GSM (gray dots) during the pre-monsoon (the left panel) and monsoon period (the right panel). (a, e) altitude (m); (b, f) air temperature T ($^{\circ}\text{C}$); (e, g) specific humidity q (g/kg); and (d, h) temporal-mean precipitation amount for the sampling dates $P\text{-mean}$ (mm/day). Notes: the colourful dots of $P\text{-mean}$ are extracted from GPCP.

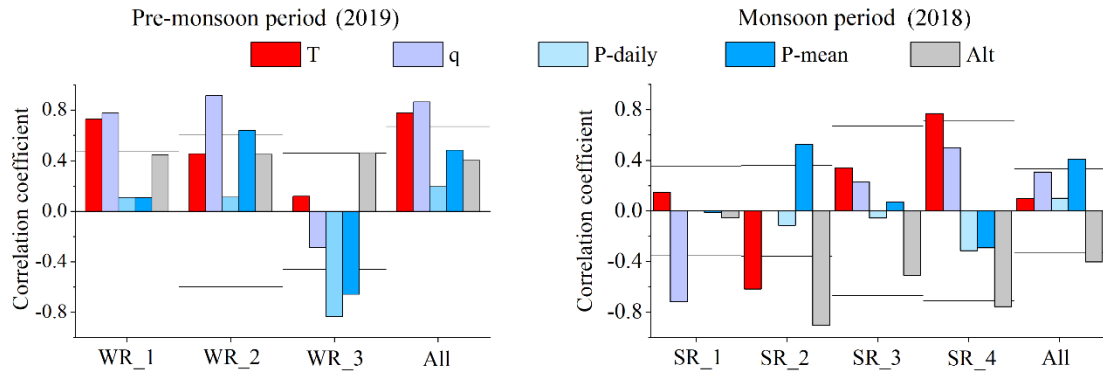


Fig.S5 Regional patterns of the correlation between $\delta^{18}\text{O}$ (a, b), d-excess (c, d) and various local factors (temperature (T), specific humidity (q), daily precipitation amount (P-daily) and temporal-mean precipitation amount for the sampling dates (P-mean), and altitude (Alt)) simulated by Iso-GSM. The left panel is for the pre-monsoon period and the right for the monsoon period. Horizontal lines indicate the correlation threshold for statistical significance ($p<0.05$).

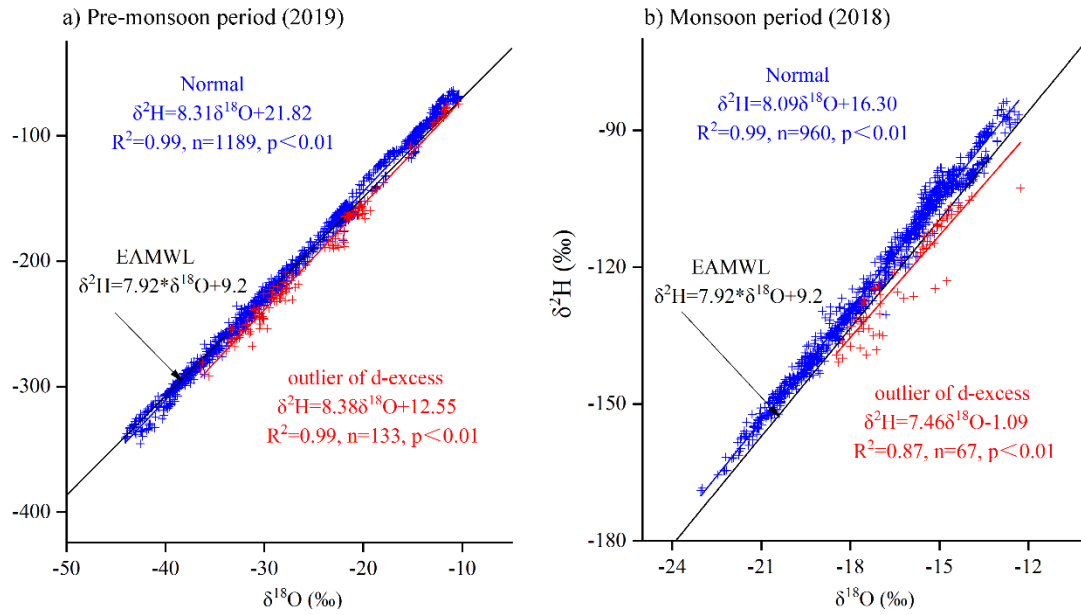


Fig. S6 $\delta^{18}\text{O}$ vs $\delta^2\text{H}$ for data with anomalous intercepts and the rest of the data used in this study, compared with the EAMWL.

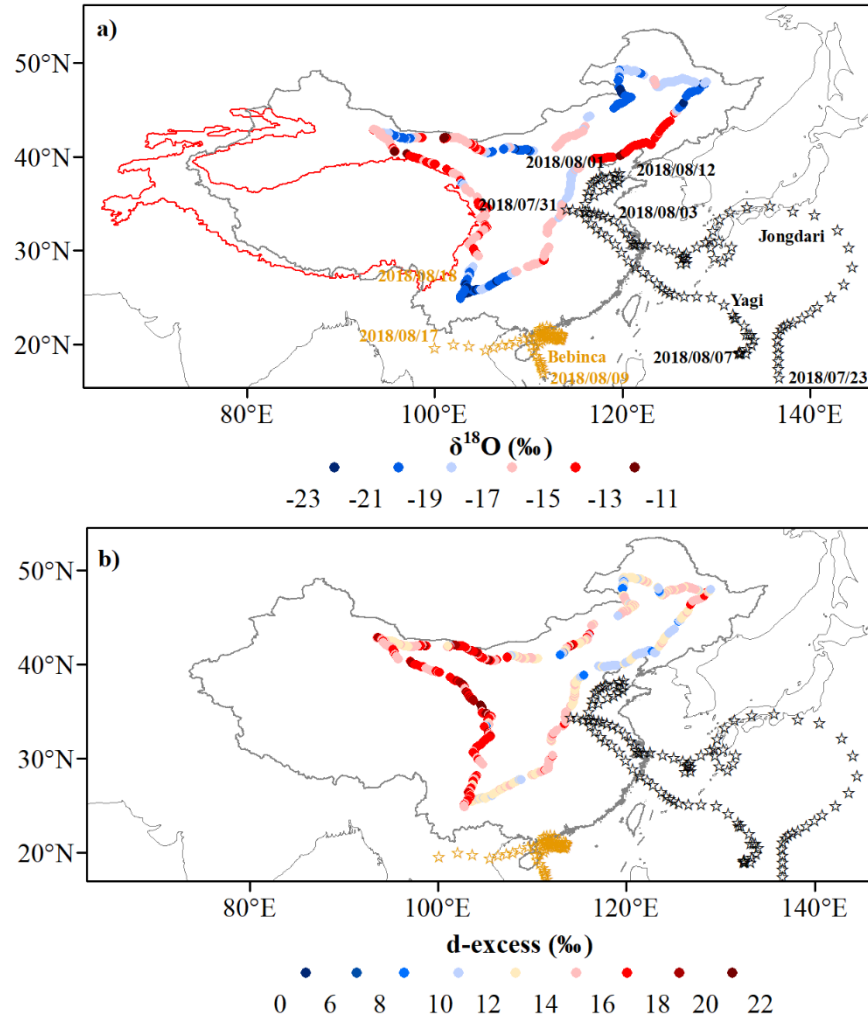


Fig.S7 Tropical cyclones that made landfall in mainland China during the 2018 monsoon observation period and the timing of tropical cyclone activity: Super typhoon Jongdari: July 23 started, August 03 arrived; Super Tropical Storm Yagi August 07 started, August 12 arrived; Super Tropical Storm Bebinca: August 09 started, August 17 arrived. (a) The bottom map shows the observed spatial distribution of $\delta^{18}\text{O}$; (b) The bottom map shows the observed spatial distribution of d-excess.

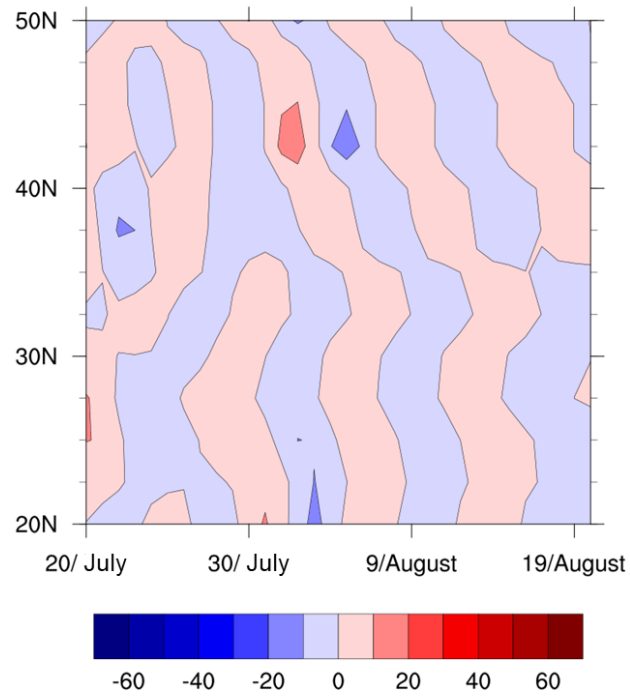


Fig.S8 Fig. Longitude averaged (100°E to 125°E) time-latitude representation (Hovmoller plot) of 5 to 10 day filtered OLR anomaly (shaded, in W/m²) during July 2018 to August.

63 II. Tables

64 **Table S1** Correlation between vapor isotopes ($\delta^{18}\text{O}$ and d-excess) and local temperature
65 (T), specific humidity (q), daily precipitation amount (P-daily), temporal-mean precipitation
66 amount for the sampling dates (P-mean) and altitude (Alt) over different regions during the
67 pre-monsoon period and monsoon period. Boldface values indicate the most significant
68 correlations ($p < 0.05$), considered the degree of freedom.

Sampling period	$\delta^{18}\text{O}$	$\delta^2\text{H}$	d	H_2O	T	q	P-daily	P-mean	Alt	
Pre-monsoon (2019)	WR_1									
	$\delta^{18}\text{O}$	1.00	1.00	0.14	0.68	0.65	0.72	0.11	0.20	0.02
	d			1.00	0.23	-0.04	0.15	0.02	0.28	-0.27
	WR_2									
	$\delta^{18}\text{O}$	1.00	1.00	0.43	0.85	0.33	0.85	-0.21	0.35	0.22
	d			1.00	0.18	0.37	0.21	0	0.15	0.47
	WR_3									
	$\delta^{18}\text{O}$	1.00	0.97	0.24	0.74	-0.38	0.75	0.47	-0.12	-0.13
	d			1.00	-0.16	-0.01	-0.17	-0.39	-0.25	-0.09
	All Zone									
	$\delta^{18}\text{O}$	1.00	1.00	0.60	0.80	0.77	0.83	0.26	0.47	0.02
	d			1.00	0.49	0.41	0.48	0.04	0.34	-0.17
Monsoon (2018)	SR_1									
	$\delta^{18}\text{O}$	1.00	1.00	0.40	0.80	-0.54	0.71	0.36	0.52	-0.26
	d			1.00	0.40	-0.23	0.43	0.27	0.57	0
	SR_2									
	$\delta^{18}\text{O}$	1.00	0.99	-0.38	0.31	-0.03	0.16	-0.13	0.08	0.23
	d			1.00	-0.28	0.22	-0.15	-0.09	-0.32	0.07
	SR_3									
	$\delta^{18}\text{O}$	1.00	0.99	-0.38	0.48	0.43	0.53	0.12	-0.48	-0.65
	d			1.00	-0.75	-0.42	-0.73	-0.21	-0.09	0.65
	SR_4									
	$\delta^{18}\text{O}$	1.00	0.99	0.35	0.87	0.58	0.87	0.44	-0.08	-0.85
	d			1.00	0.44	0.46	0.41	0.08	0.07	-0.49
All Zone										
$\delta^{18}\text{O}$	1.00	0.99	0.10	0.20	0.32	0.22	0.10	-0.15	-0.16	
d			1.00	-0.33	0	-0.28	-0.02	-0.12	0.39	

69

70

Table S2 The degree of freedom D (reserved as integer) and threshold for the correlation coefficient to be statistically significant at 95% (r).

Sampling period	Region	Degree of freedom D	r
Pre-monsoon (2019)	WR_1	16	0.47
	WR_2	9	0.60
	WR_3	17	0.46
	All	7	0.67
Monsoon (2018)	SR_1	32	0.35
	SR_2	28	0.36
	SR_3	7	0.67
	SR_4	6	0.71
	All	36	0.33

Table S3 Correlation coefficients and slopes of the relationship between observed and simulated $\delta^{18}\text{O}$, temperature (T), specific humidity (q), daily precipitation amount (P-daily) and temporal-mean precipitation amount for the ssampling dates (P-mean) from Iso-GSM. Boldface values indicate the most significant correlations ($p < 0.05$), considered the degree of freedom.

		r	Slope
Pre-monsoon (2019)	$\delta^{18}\text{O}$	0.84	0.61
	d-excess	0.16	0.10
	T	0.87	0.70
	q	0.84	0.70
	P-daily	0.2	0.13
	P-mean	0.63	1.05
Monsoon (2018)	$\delta^{18}\text{O}$	0.24	0.25
	d-excess	0.15	0.13
	T	0.46	0.32
	q	0.85	0.89
	P-daily	0.18	0.15
	P-mean	0.66	0.79

III. Text

(1) Method to estimate the degree of freedom of time series

The statistical significance of correlation coefficients between two time series depends on the degree of freedom D of these time series. If the samples of the time series are all independent from each other, then $D=N-2$, where N is the number of samples.

Our time series evolves smoothly, therefore consecutive samples are not completely independent from each other. For example, the i th sample is typically intermediate between the $(i-1)$ th sample and the $(i+1)$ th sample.

Therefore, to estimate the degree of freedom D , we need to know what is the typical duration between 2 samples (η), that ensures that the 2 samples are independent. η is called the auto-correlation time scale.

D can be calculated as: $D= T/\eta$

where T is the duration of the sampling period (e.g. 24 days during the pre-monsoon period)

A similar approach was followed in Roca et al 2010.

We estimate η for each time series X ($\delta^{18}\text{O}$ or d-excess) for each season and region. Here is an example for all regions of the pre-monsoon period:

* We have 1189 samples averaged to a 10-min temporal resolution . We therefore have a time series that is evenly sampled in time. For each lag l from -6h to +6h, with a spacing of 1 hour, we calculate the correlation r between the time series X and the same time series lagged by l . For example, if $l=0$, then this is the correlation between X and itself, so it is 1. As l increases, the correlation decreases and tends to 0.

* Then we plot $-\ln(r)$ as a function of $|l|$. We find a linear relationship with slope s . For example in this case, we find a slope of 0.0342 hour^{-1} .

* we calculate η as $1/s$. For example in this case, we find $\eta=1/0.0342=29.24$.

* Calculate $D= T/\eta =1189/6/29.24=6.77$. Note: 1189 samples have a 10-min temporal resolution, and we select the l with a 1 hour temporal resolution, so here we divide by 6.

* The same calculation of the degree of freedom have been done for each period/region and each season.

Roca, R., Chambon, P., Jobard, I., Kirstetter, P. E., Gosset, M., & Bergès, J. C. (2010). Comparing satellite and surface rainfall products over West Africa at meteorologically relevant scales during the AMMA campaign using error estimates. *Journal of Applied Meteorology and Climatology*, 49(4), 715-731.

(2) Method to make the altitude correction for the outputs of Iso-GSM:

In observations, altitude varies at short spatial scales as the route goes up and down hills. This contributes to δ variations. IsoGSM, as a coarse resolution global model, cannot capture such small-scale variations of altitude. We thus need to correct for the altitude difference between observations and isoGSM.

At each location, the altitude corrected isoGSM δ , δ_{corr} , is calculated as:

$$\delta_{\text{corr}} = \delta_{\text{Iso-GSM}} + a_{\text{alt}} * (\text{Alt}_{\text{obs}} - \text{Alt}_{\text{Iso-GSM}})$$

where $\delta_{\text{Iso-GSM}}$ is the original output of iso-GSM, a_{alt} is the slope of $\delta_{\text{Iso-GSM}}$ as a function of altitude used in iso-GSM ($\text{Alt}_{\text{Iso-GSM}}$), and Alt_{obs} is the measured altitude by our portable GPS unit.

Because the relationship between δ and altitude is significant only during the monsoon season, we apply this correction only for the outputs during the monsoon season.

We found that $\text{Alt}_{\text{Iso-GSM}}$ is higher than Alt_{obs} in the southwest corner of China (Fig S6). This tends to make $\delta_{\text{Iso-GSM}}$ more depleted compared to observations. The altitude correction partially corrects this bias (Fig SIII-1). In addition, the correlation between the simulated $\delta^{18}\text{O}$ and measured $\delta^{18}\text{O}$ is improved from 0.09 to 0.24, due to the account for the small-scale variations in altitude.

Only $\delta^{18}\text{O}$ and $\delta^2\text{H}$ during the monsoon period are strongly correlated with altitude in the Iso-GSM simulations, with $r=0.79$ and $r=0.80$ ($n=960$, $p<0.01$, considered the degree of freedom), respectively. So no altitude corrections were made for the other parameters and the simulations during the pre-monsoon period.

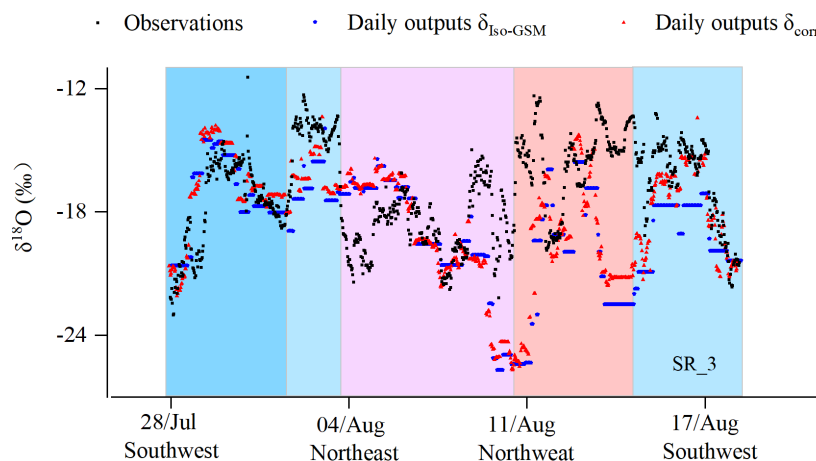


Fig SIII-1. Comparison of the observed vapor $\delta^{18}\text{O}$ (observations) with that simulated at the daily scale by Iso-GSM, without the altitude correction ($\delta_{\text{Iso-GSM}}$) and with the correction (δ_{corr}).